

# Hybrid Parametric Classes of Isotropic Covariance Functions for Spatial Random Fields

Alfredo Alegría\*<sup>1</sup>, Fabián Ramírez<sup>1</sup>, and Emilio Porcu<sup>2</sup>

<sup>1</sup>Departamento de Matemática, Universidad Técnica Federico Santa María, Chile

<sup>2</sup>Department of Mathematics, Khalifa University, The Arab Emirates

January 16, 2023

## Abstract

Covariance functions are the core of spatial statistics, stochastic processes, machine learning as well as many other theoretical and applied disciplines. The properties of the covariance function at small and large distances determine the geometric attributes of the associated Gaussian random field. Having covariance functions that allow to specify both local and global properties is certainly on demand. This paper provides a method to find new classes of covariance functions having such properties. We term these models *hybrid* as they are obtained as scale mixtures of piecewise covariance kernels against measures that are also defined as piecewise linear combination of parametric families of measures. In order to illustrate our methodology, we provide new families of covariance functions that are proved to be richer with respect to other well known families that have been proposed by earlier literature. More precisely, we derive a hybrid Cauchy-Matérn model, which allows us to index both long memory and mean square differentiability of the random field, and a hybrid Hole-Effect-Matérn model, which is capable of attaining negative values (hole effect), while preserving the local attributes of the traditional Matérn model. Our findings are illustrated through numerical studies with both simulated and real data.

*Keywords:* Cauchy model; Gaussian scale mixtures; Hole effect; Long memory; Matérn model; Mean square differentiability.

## 1 Introduction

Covariance functions are central to many disciplines such as spatial statistics (Cressie, 1993; Chilès and Delfiner, 2012; Hristopulos, 2020), stochastic processes (Porcu et al., 2018a,b), machine learning (Schaback and Wendland, 2006; James et al., 2013; Barp et al., 2022), numerical analysis (Pazouki and Schaback, 2011; Cockayne et al., 2019) and stochastic mechanics (Ostoja-Starzewski, 2006, with the references therein). Recent applications in climatology (Guinness and Hammerling, 2018; Edwards et al., 2019), oceanography (Furrer et al., 2007; Di Lorenzo et al., 2014), environmental sciences (Cressie and Kornak, 2003; Stein, 2007) and natural resources engineering (Chen et al., 2018; Emery and Séguret, 2020) witness on the importance of covariance functions.

It is very customary to assume the covariance function to depend on the distance between any pair of random variables located at two different points at the input space. Such an assumption is

---

\*Corresponding author. Email: alfredo.alegria@usm.cl

termed isotropy in spatial statistics and machine learning, and it is termed radial symmetry in other areas of applied mathematics. The behaviour of the covariance function at short or long distances (we call this local and global properties, respectively) is crucial to understand the properties of random processes with a given covariance function. Specifically, the local properties are related to the fractal dimension as well as the geometric properties (e.g., mean square differentiability) of the associated random process, as well as to its sample paths. On the other hand, the global behaviour of the covariance function allows to characterize persistency or antipersistency (i.e., the long term behaviour) of the associated process. Another global behaviour of great interest is the so-called hole effect, which means that the covariance function could take negative values in a certain interval.

Finding parametric families of isotropic covariance functions that allow to index both local and global behaviour is a major challenge that has been tackled to a very limited extent. The Matérn family has been the cornerstone in spatial statistics for over half a century now (Stein, 1999). Its popularity is due to a parameter that controls the degree of mean square differentiability and fractal dimension of the corresponding random field (Stein, 1999). Recently, Bevilacqua et al. (2022) have shown that the Matérn class is a special case of a richer class of models that, additionally to indexing local properties, allow to switch between compact or global supports. In turn, compactly supported models lead to sparse covariance matrices (Furrer et al., 2006; Kaufman et al., 2008) and this implies considerable computational gains in both estimation and prediction. Unfortunately, the Matérn class does not allow to index global behaviour of the associated random process. The Generalized Cauchy family (Gneiting and Schlather, 2004) allows to index the fractal dimension and the long memory behaviour. Notably, it does not allow to index mean square differentiability, as the model is either non differentiable or infinitely differentiable at the origin. The same properties are shared by the Dagum model (Berg et al., 2008), which does not allow to index mean square differentiability either. None of the aforementioned models allow to attain negative spatial dependencies.

Spectral approaches can be a promising avenue to find flexible families of covariance functions. Laga and Kleiber (2017) proposed a modified version of the spectral density associated with the Matérn family. The new class has two additional parameters that can be loosely interpreted as a continuous version of a moving average process. More recently, Ma and Bhadra (2022) have proved that a two-fold application of Gaussian scale mixtures can provide models with polynomial decays while preserving the local properties of the candidate covariance function. Other non conventional properties of covariance functions have been studied by Alegría (2020) and Alegría et al. (2021), who proposed some modified scale mixtures representations to obtain classes of cross-covariance functions with non-monotonic behaviours (the so-called cross-dimple effect) for vector-valued random fields. In Schlather and Moreva (2017), models that allow for a smooth transition between stationary and intrinsically stationary Gaussian random fields are derived.

All the previously mentioned parametric classes of covariance functions admit a scale mixture representation of a Gaussian kernel against a continuous, positive and bounded measure. Our paper starts from the Schoenberg integral representation of isotropic covariance functions on  $\mathbb{R}^d$  (Schoenberg, 1938), for all natural numbers,  $d$ . We specifically assume the Schoenberg measures to be parametric families of measures that are defined piecewise. Such a strategy is then shown to provide hybrid classes that generalize classes proposed in earlier literature. We illustrate this methodology by constructing a model that combines the global attributes of the Cauchy class and the local properties of the Matérn class. We show that the proposed model admits a closed form expression and examine its theoretical properties. Additionally, we study a more flexible formulation, where the Gaussian kernel involved in the scale mixture is replaced with a covariance kernel that is also defined piecewise. Following this approach, we derive a hybrid model with local

behaviour of Matérn type, and global behaviour that allows for covariance functions with negative values. We conduct numerical experiments with both simulated and real data in order to assess the statistical performance of the proposed models.

The article is organized as follows. Section 2 contains a concise review of random fields and covariance functions coming from scale mixtures. Section 3 presents general methodologies to build hybrid covariance models. Then, we derive the hybrid Cauchy-Matérn and the hybrid Hole-Effect-Matérn classes. Section 4 guides the reader through some numerical studies. We finally provide a critical discussion in Section 5, including a description of technical extensions of the present work such as the multivariate case, where covariance functions are matrix-valued, and the case of spherically indexed fields, where isotropy is defined in terms of the geodesic distance.

## 2 Background

Let  $\{Z(\mathbf{s}) : \mathbf{s} \in \mathbb{R}^d\}$  be a (centered) second-order stationary Gaussian random field on  $\mathbb{R}^d$ . Such a field is completely characterized by its covariance function (or kernel). The isotropy of the covariance function is defined through a mapping  $\varphi : [0, \infty) \rightarrow \mathbb{R}$  such that  $\text{cov}[Z(\mathbf{s}), Z(\mathbf{s}')] = \varphi(h)$ , for every  $\mathbf{s}, \mathbf{s}' \in \mathbb{R}^d$ , where  $h = \|\mathbf{s} - \mathbf{s}'\|$ . The covariance function must satisfy the positive (semi) definiteness condition: for any  $k \in \mathbb{N}$ ,  $\{a_1, \dots, a_k\} \subset \mathbb{R}$  and  $\{\mathbf{s}_1, \dots, \mathbf{s}_k\} \subset \mathbb{R}^d$ ,

$$\sum_{i,j=1}^k a_i a_j \varphi(\|\mathbf{s}_i - \mathbf{s}_j\|) \geq 0.$$

We use the notation  $\varphi(\cdot; \boldsymbol{\lambda})$  for a parametric family of continuous covariance functions, where  $\boldsymbol{\lambda} \in \mathbb{R}^p$  is a vector of parameters. Further, we make use of the celebrated Schoenberg' theorem (Schoenberg, 1938): the functions  $\varphi$  that are valid in any dimension  $d \in \mathbb{N}$  are uniquely written as Gaussian scale mixtures of positive and bounded measures, that is

$$\varphi(h; \boldsymbol{\lambda}) = \int_0^\infty \exp(-uh^2) G(du; \boldsymbol{\lambda}), \quad h \geq 0,$$

where  $\{G(\cdot; \boldsymbol{\lambda}), \boldsymbol{\lambda} \in \mathbb{R}^p\}$  is a parametric family of measures, that are termed Schoenberg measures in Daley and Porcu (2014). Most of the covariance classes listed in the introduction admit such a representation against a measure that is absolutely continuous with respect to the Lebesgue measure, that is

$$\varphi(h; \boldsymbol{\lambda}) = \int_0^\infty \exp(-uh^2) g(u; \boldsymbol{\lambda}) du, \quad h \geq 0, \quad (2.1)$$

for  $\{g(\cdot; \boldsymbol{\lambda}), \boldsymbol{\lambda} \in \mathbb{R}^p\}$  a parametric family of nonnegative functions. Throughout, we call  $g$  the mixing function.

We now describe examples of some parametric classes of functions  $\varphi$  that are determined according to (2.1). Special attention is devoted to the Matérn, Cauchy and Generalized Cauchy models. Other examples, including the stable and generalized hyperbolic models, can be found in Yaglom (1987), Barndorff-Nielsen (1978), Schlather (2010) and Porcu et al. (2018b).

**Example 2.1** (Matérn). This class of covariance functions is defined as (Matérn, 1986)

$$\varphi_{\mathcal{M}}(h; \boldsymbol{\lambda}) = \frac{2^{1-\nu}}{\Gamma(\nu)} (h/\alpha)^\nu K_\nu(h/\alpha), \quad h \geq 0, \quad (2.2)$$

where  $\Gamma$  is the gamma function and  $K_\nu$  is the modified Bessel function of the second kind (Abramowitz and Stegun, 1972). Here,  $\boldsymbol{\lambda} = [\alpha, \nu]^\top$ , with  $\alpha$  and  $\nu$  being positive parameters that control the scale (the rate of decay of the covariance in terms of  $h$ ) and shape of (2.2), respectively. More precisely,  $\nu$  regulates the degree of mean square differentiability of the random field (large values of  $\nu$  are associated with smoother sample paths) (Stein, 1999). When  $\boldsymbol{\lambda} = [\alpha, 1/2]^\top$ , (2.2) simplifies into the exponential model,  $\exp(-h/\alpha)$ . On the other hand, as  $\nu \rightarrow \infty$ , a reparameterization of (2.2) tends to the Gaussian covariance function, defined as  $\exp(-h^2/\alpha)$ .

**Example 2.2** (Cauchy). This class of covariance functions is given by (Chilès and Delfiner, 2012)

$$\varphi_C(h; \boldsymbol{\lambda}) = (1 + h^2/\alpha)^{-\nu/2}, \quad h \geq 0, \quad (2.3)$$

with  $\boldsymbol{\lambda} = [\alpha, \nu]^\top$ . As in the Matérn model,  $\alpha > 0$  is a scale parameter. However, unlike the Matérn model which decays exponentially with distance (Stein, 1999), (2.3) has a polynomial decay regulated by  $\nu > 0$ . When  $\nu \in (0, 2)$ , such a polynomial decay is connected with the Hurst parameter, a measure of long term memory, given by  $H = 1 - \nu/2$ .

**Example 2.3** (Generalized Cauchy). This class of covariance functions is defined as (Gneiting and Schlather, 2004 and the references therein)

$$\varphi_{GC}(h; \boldsymbol{\lambda}) = \left(1 + h^\delta/\alpha\right)^{-\nu/\delta}, \quad h \geq 0, \quad (2.4)$$

with  $\boldsymbol{\lambda} = [\alpha, \nu, \delta]^\top$ , where  $\delta \in (0, 2]$ ,  $\alpha > 0$  and  $\nu > 0$ . This generalized class preserves the polynomial decay of (2.3), but it is more flexible in the sense that the fractal dimension can be arbitrarily regulated through  $\delta$  (see Gneiting and Schlather, 2004 for details). Maybe surprisingly, this model does not allow to control the mean square differentiability of the respective random field, as the model is either non differentiable or infinitely differentiable at the origin.

Additional classes of covariance functions can be obtained from the more general mixture

$$\varphi(h; \boldsymbol{\lambda}, \boldsymbol{\vartheta}) = \int_0^\infty \phi(h; u, \boldsymbol{\vartheta})g(u; \boldsymbol{\lambda})du, \quad h \geq 0, \quad (2.5)$$

where  $\phi(\cdot; u, \boldsymbol{\vartheta})$  is an arbitrary covariance kernel, for every  $u > 0$ , and  $\boldsymbol{\vartheta}$  is a vector of parameters. Since the class of positive definite functions is a convex cone that is closed under the topology of pointwise convergence, if  $\phi$  is valid (positive definite) in  $\mathbb{R}^d$  for  $d \leq d'$ , for some  $d' \in \mathbb{N}$ , then  $\varphi$  is valid in  $\mathbb{R}^d$  for  $d \leq d'$  as well. We refer the reader to Emery and Lantuéjoul (2006) for several explicit examples.

## 3 Hybrid Classes of Covariance Functions

### 3.1 General Construction

In this study, we propose new parametric classes of isotropic covariance functions,  $\tilde{\varphi}(\cdot; \boldsymbol{\lambda}, \boldsymbol{\omega}, \boldsymbol{\xi})$ , determined according to

$$\tilde{\varphi}(h; \boldsymbol{\lambda}, \boldsymbol{\omega}, \boldsymbol{\xi}) = \omega_1 \int_0^{\xi_1} \exp(-uh^2)g_1(u; \boldsymbol{\lambda}_1)du + \omega_2 \int_{\xi_2}^\infty \exp(-uh^2)g_2(u; \boldsymbol{\lambda}_2)du, \quad (3.1)$$

where  $g_1$  and  $g_2$  are nonnegative functions on  $[0, \xi_1)$  and  $[\xi_2, \infty)$ , respectively, and  $\boldsymbol{\lambda} = [\boldsymbol{\lambda}_1^\top, \boldsymbol{\lambda}_2^\top]^\top$ ,  $\boldsymbol{\omega} = [\omega_1, \omega_2]^\top$  and  $\boldsymbol{\xi} = [\xi_1, \xi_2]^\top$  are vectors of parameters, with  $\omega_i, \xi_i > 0$ , for  $i = 1, 2$ . In other

words, we replace the mixing function,  $g$ , in Equation (2.1) with a function  $\tilde{g}$  that is defined piecewise, i.e.,

$$\tilde{g}(u; \boldsymbol{\lambda}, \boldsymbol{\omega}, \boldsymbol{\xi}) = \omega_1 g_1(u; \boldsymbol{\lambda}_1) 1_{[0, \xi_1)}(u) + \omega_2 g_2(u; \boldsymbol{\lambda}_2) 1_{[\xi_2, \infty)}(u), \quad u \geq 0, \quad (3.2)$$

with  $1_A(\cdot)$  standing for the indicator function of a set  $A$ . Note that  $\tilde{g}$  may have discontinuities as it is built by gluing two individual pieces. If the functions  $g_i$  are continuous and bounded on their domains, a direct application of the dominated convergence theorem implies that the proposed covariance function (3.1) is continuous on  $[0, \infty)$ . Throughout this manuscript, each function  $g_i$  is positively proportional to a continuous probability density function. Hence, the parametric family proposed in Equation (3.1) belongs to the Schoenberg class as defined through Equation (2.1).

A more general construction considers different kernels in each segment of the mixture, i.e.,

$$\tilde{\varphi}(h; \boldsymbol{\lambda}, \boldsymbol{\omega}, \boldsymbol{\xi}, \boldsymbol{\vartheta}) = \omega_1 \int_0^{\xi_1} \phi_1(h; u, \boldsymbol{\vartheta}_1) g_1(u; \boldsymbol{\lambda}_1) du + \omega_2 \int_{\xi_2}^{\infty} \phi_2(h; u, \boldsymbol{\vartheta}_2) g_2(u; \boldsymbol{\lambda}_2) du, \quad (3.3)$$

where  $\boldsymbol{\vartheta} = [\boldsymbol{\vartheta}_1^\top, \boldsymbol{\vartheta}_2^\top]^\top$ . If  $\phi_i$  is a valid covariance function in  $\mathbb{R}^d$  for  $d \leq d'_i$ , for some  $d'_i \in \mathbb{N}$ ,  $i = 1, 2$ , then (3.3) is a valid model in  $\mathbb{R}^d$  if and only if  $d \leq \min(d'_1, d'_2)$ . The continuity of (3.3) can be justified by following the same arguments used for the continuity of (3.1).

**Remark 3.1.** Let us point out some additional remarks on this methodology.

1. When  $\xi_1 = \xi_2 = \xi$ , this parameter produces a continuous bridge between two apparently disunited *marginal* models. More precisely, as it increases from 0 to  $\infty$ , we gradually go from  $\omega_2 \int_0^{\infty} \phi_2(h; u, \boldsymbol{\vartheta}_2) g_2(u; \boldsymbol{\lambda}_2) du$  to  $\omega_1 \int_0^{\infty} \phi_1(h; u, \boldsymbol{\vartheta}_1) g_1(u; \boldsymbol{\lambda}_1) du$ .
2. When  $\xi_1 > \xi_2$ , instead, there is a superposition of the marginal structures in the interval  $[\xi_2, \xi_1)$ . As  $\xi_2 \rightarrow 0$  and  $\xi_1 \rightarrow \infty$ , we obtain the greatest possible superposition, which corresponds to a linear combination of the marginal models,  $\omega_1 \int_0^{\infty} \phi_1(h; u, \boldsymbol{\vartheta}_1) g_1(u; \boldsymbol{\lambda}_1) du + \omega_2 \int_0^{\infty} \phi_2(h; u, \boldsymbol{\vartheta}_2) g_2(u; \boldsymbol{\lambda}_2) du$ .

The apparent flexibility of the proposed mixtures is justified by classical theory on local and global behaviour of covariance functions. In particular, a direct application of Tauberian theorems (Stein, 1999) proves that mean square differentiability of  $\tilde{\varphi}$  will be determined by  $g_2$ . On the other hand, direct inspection in concert with Equation (4) in Gneiting and Schlather (2004) shows that the long term behaviour of  $\tilde{\varphi}$  is decided by  $g_1$ . The next sections show that it is possible to provide examples in algebraically closed form that allow to attain the desired flexibility.

### 3.2 A Hybrid Cauchy-Matérn Class

We present a hybrid Cauchy-Matérn model, for which the acronym  $\mathcal{CM}$  is used. This model is a special case of (3.1). Let us first introduce the generalized incomplete gamma function (Chaudhry and Zubair, 1994),

$$\Gamma(a; b; c) = \int_b^{\infty} t^{a-1} \exp(-t - ct^{-1}) dt,$$

and the lower incomplete gamma function,  $\gamma(a, b) = \Gamma(a; 0; 0) - \Gamma(a; b; 0)$ .

**Proposition 3.1.** Let  $\boldsymbol{\lambda} = [\boldsymbol{\lambda}_1^\top, \boldsymbol{\lambda}_2^\top]^\top$ , with  $\boldsymbol{\lambda}_i = [\alpha_i, \nu_i]^\top$ ,  $\boldsymbol{\omega} = [\omega_1, \omega_2]^\top$  and  $\boldsymbol{\xi} = [\xi_1, \xi_2]^\top$  be vectors having positive elements. Let

$$\tilde{\varphi}_{\mathcal{CM}}(h; \boldsymbol{\lambda}, \boldsymbol{\omega}, \boldsymbol{\xi}) = \omega_1 \tilde{\varphi}_{\mathcal{C}}^{(1)}(h; \boldsymbol{\lambda}_1, \xi_1) + \omega_2 \tilde{\varphi}_{\mathcal{M}}^{(2)}(h; \boldsymbol{\lambda}_2, \xi_2), \quad h \geq 0, \quad (3.4)$$

where

$$\tilde{\varphi}_{\mathcal{C}}^{(1)}(h; \boldsymbol{\lambda}_1, \xi_1) = \frac{\gamma(\nu_1/2, (h^2 + \alpha_1)\xi_1)}{\Gamma(\nu_1/2)} \varphi_{\mathcal{C}}(h; \boldsymbol{\lambda}_1) \quad (3.5)$$

and

$$\tilde{\varphi}_{\mathcal{M}}^{(2)}(h; \boldsymbol{\lambda}_2, \xi_2) = \varphi_{\mathcal{M}}(h; \boldsymbol{\lambda}_2) - \frac{1}{\Gamma(\nu_2)} \Gamma\left(\nu_2; \frac{1}{4\xi_2\alpha_2^2}; \frac{h^2}{4\alpha_2^2}\right), \quad (3.6)$$

with  $\varphi_{\mathcal{M}}$  and  $\varphi_{\mathcal{C}}$  being, respectively, the Matérn and the Cauchy models defined at (2.2) and (2.3). Then,  $\tilde{\varphi}_{\mathcal{C}\mathcal{M}}$  is positive definite in  $\mathbb{R}^d$  for all  $d \in \mathbb{N}$ .

**Proof 3.1.** We provide a proof of the constructive type, by showing that  $\tilde{\varphi}_{\mathcal{C}\mathcal{M}}$  admits the representation (3.1), with  $g_1(u; \boldsymbol{\lambda}_1) = g_{\mathcal{C}}(u; \boldsymbol{\lambda}_1)$  and  $g_2(u; \boldsymbol{\lambda}_2) = g_{\mathcal{M}}(u; \boldsymbol{\lambda}_2)$ , with  $g_{\mathcal{C}}$  and  $g_{\mathcal{M}}$  that are respectively defined as

$$g_{\mathcal{C}}(u; \boldsymbol{\lambda}_1) = \frac{\alpha_1^{\nu_1/2}}{\Gamma(\nu_1/2)} u^{\nu_1/2-1} \exp(-\alpha_1 u), \quad (3.7)$$

and

$$g_{\mathcal{M}}(u; \boldsymbol{\lambda}_2) = \frac{1}{\Gamma(\nu_2)} \left(\frac{1}{2\alpha_2}\right)^{2\nu_2} u^{-\nu_2-1} \exp\left(-\frac{1}{4u\alpha_2^2}\right), \quad (3.8)$$

where for both cases all the parameters are positive. To attain the analytical expression of  $\tilde{\varphi}_{\mathcal{C}}^{(1)}$ , we notice that

$$\begin{aligned} \int_0^{\xi_1} \exp(-uh^2) g_{\mathcal{C}}(u; \boldsymbol{\lambda}_1) du &= \varphi_{\mathcal{C}}(h; \boldsymbol{\lambda}_1) \int_0^{\xi_1} \frac{(h^2 + \alpha_1)^{\nu_1/2}}{\Gamma(\nu_1/2)} u^{\nu_1/2-1} \exp(-(h^2 + \alpha_1)u) du \\ &= \varphi_{\mathcal{C}}(h; \boldsymbol{\lambda}_1) \frac{\gamma(\nu_1/2, (h^2 + \alpha_1)\xi_1)}{\Gamma(\nu_1/2)}, \end{aligned}$$

where the second equality is due to the fact that the integral on the right hand side of the first line amounts to the cumulative distribution function of a gamma random variable with parameters  $h^2 + \alpha_1$  and  $\nu_1/2$ .

To attain the expression of  $\tilde{\varphi}_{\mathcal{M}}^{(2)}$ , we invoke Equation (10) in Alegría et al. (2021), so that

$$\int_0^{\xi_2} \exp(-uh^2) g_{\mathcal{M}}(u; \boldsymbol{\lambda}_2) du = \frac{1}{\Gamma(\nu_2)} \Gamma\left(\nu_2; \frac{1}{4\xi_2\alpha_2^2}; \frac{h^2}{4\alpha_2^2}\right). \quad (3.9)$$

The function  $\tilde{\varphi}_{\mathcal{M}}^{(2)}$  is thus attained by invoking formula 3.471.9 in Gradshteyn and Ryzhik (2007), for which we have  $\int_0^{\infty} \exp(-uh^2) g_{\mathcal{M}}(u; \boldsymbol{\lambda}_2) du = \varphi_{\mathcal{M}}(h; \boldsymbol{\lambda}_2)$ .  $\square$

When  $\nu_2 = n + 1/2$ , for some  $n \in \mathbb{N}$ , (3.6) can be expressed in terms of complementary error functions and modified Bessel functions of first and second kinds. We refer the reader to Alegría et al. (2021) for a more detailed study of these special cases.

The flexibility of the proposed structure is now illustrated through the following result, where we use the notation  $f_1(h) \sim f_2(h)$ ,  $h \rightarrow \infty$ , to represent that, for some positive constant  $c_0$ , the asymptotic relationship  $\lim_{h \rightarrow \infty} f_1(h)/f_2(h) = c_0$  holds.

**Proposition 3.2.** Let  $Z$  be a Gaussian random field with covariance function of the form (3.4). Then,  $Z$  is  $\kappa$ -times mean square differentiable if and only if  $\nu_2 > \kappa \geq 0$ . Moreover, it is true that  $\tilde{\varphi}_{\mathcal{C}\mathcal{M}}(h; \boldsymbol{\lambda}, \boldsymbol{\omega}, \boldsymbol{\xi}) \sim h^{-\nu_1}$ ,  $h \rightarrow \infty$ . Hence, the Hurst parameter associated with  $Z$  is solely indexed by the parameter  $\nu_1$ .

**Proof 3.2.** Arguments in Chapter 2 of Stein (1999) show that an isotropic random field with covariance function  $\varphi$  is  $\kappa$ -times mean square differentiable if and only if  $\varphi^{(2\kappa)}(0; \boldsymbol{\lambda})$  exists and is finite. Direct inspection in concert with dominated convergence on the invoked Schoenberg representation (2.1) show that this happens if and only if the mixing function  $g$  satisfies

$$\int_0^\infty u^\kappa g(u; \boldsymbol{\lambda}) du < \infty. \quad (3.10)$$

We use the latter argument for the special case of the function  $\tilde{\varphi}_{\mathcal{CM}}$ , for which the tale of the resulting mixing function is uniquely determined by the mixing function associated with  $\varphi_{\mathcal{M}}^{(2)}$  as in Proposition 3.1. Direct inspection shows that (3.10) is true if and only if  $\nu_2 > \kappa$ . The first part of the proposition is established.

For the second part, note that (3.5) behaves as  $h^{-\nu_1}$ , as  $h \rightarrow \infty$ , because the lower incomplete gamma function involved in such an equation tends to  $\Gamma(\nu_1/2)$ , and the Cauchy class with parameter  $\nu_1$  decays as  $h^{-\nu_1}$ . The result follows by noting that (3.6) is dominated by the traditional Matérn model, which decays exponentially.  $\square$

To wrap up, the hybrid Cauchy-Matérn model allows to index both mean square differentiability and long term behaviour of the associated Gaussian random field. We also note that these properties are independently addressed by the two parameters  $\nu_1$  and  $\nu_2$ , and hence those parameters are statistically identifiable and allow to decouple local and global properties.

From a statistical viewpoint, a parsimonious choice may be considered by setting  $\omega_1 = \omega_2 = \omega$ ,  $\alpha_1 = \alpha_2 = \alpha$  and  $\xi_1 = \xi_2 = \xi$ . Thus, we obtain that Proposition 3.1 provides a five parameter family where  $\omega$  indexes the variance,  $\alpha$  the scale,  $\nu_2$  the mean square differentiability, and  $\nu_1$  the Hurst effect, whereas  $\xi$  is a parameter that balances the shapes of the marginal structures involved in this model. Hence, (3.4) generalizes the Matérn model in that it allows for polynomial decay while indexing continuously mean square differentiability.

Figure 3.1 shows the parsimonious hybrid Cauchy-Matérn model for different values of  $\xi$ . The traditional Matérn and traditional Cauchy, as well as their average, which are also special cases of the hybrid construction, are reported for comparison purposes. Note that the curves have a linear or parabolic decay near the origin according to  $\nu_2 = 1/2$  or  $\nu_2 = 3/2$ , respectively, and then the decay is more gradual (polynomial rate) for large distances according to  $\nu_1$ , which is consistent with the local and global patterns that are coexisting. We observe that  $\xi$  has a manifest impact on the shape of the covariance function, as it produces some interesting forms (apparent changes of concavity) that could be useful in practice.

### 3.3 A Hybrid Hole-Effect-Matérn Class

We now present a hybrid class of covariance functions, with local attributes of Matérn type, attaining negative values at large distances. We use the acronym  $\mathcal{HM}$  for this model, termed hybrid Hole-Effect-Matérn. The proposed class comes from the mixture (3.3), where  $\phi_1$  is chosen in such a way that the resulting model can take negative values.

**Proposition 3.3.** Let  $\boldsymbol{\lambda} = [\boldsymbol{\lambda}_1^\top, \boldsymbol{\lambda}_2^\top]^\top$ , with  $\boldsymbol{\lambda}_i = [\alpha_i, \nu_i]^\top$ ,  $\boldsymbol{\omega} = [\omega_1, \omega_2]^\top$  and  $\boldsymbol{\xi} = [\xi_1, \xi_2]^\top$  be vectors having positive elements, and  $\boldsymbol{\vartheta} = [\tau, \eta]^\top$  be a vector of additional parameters. Let

$$\tilde{\varphi}_{\mathcal{HM}}(h; \boldsymbol{\lambda}, \boldsymbol{\omega}, \boldsymbol{\xi}, \boldsymbol{\vartheta}) = \omega_1 \tilde{\varphi}_{\mathcal{H}}^{(1)}(h; \boldsymbol{\lambda}_1, \xi_1, \boldsymbol{\vartheta}) + \omega_2 \tilde{\varphi}_{\mathcal{M}}^{(2)}(h; \boldsymbol{\lambda}_2, \xi_2), \quad h \geq 0, \quad (3.11)$$

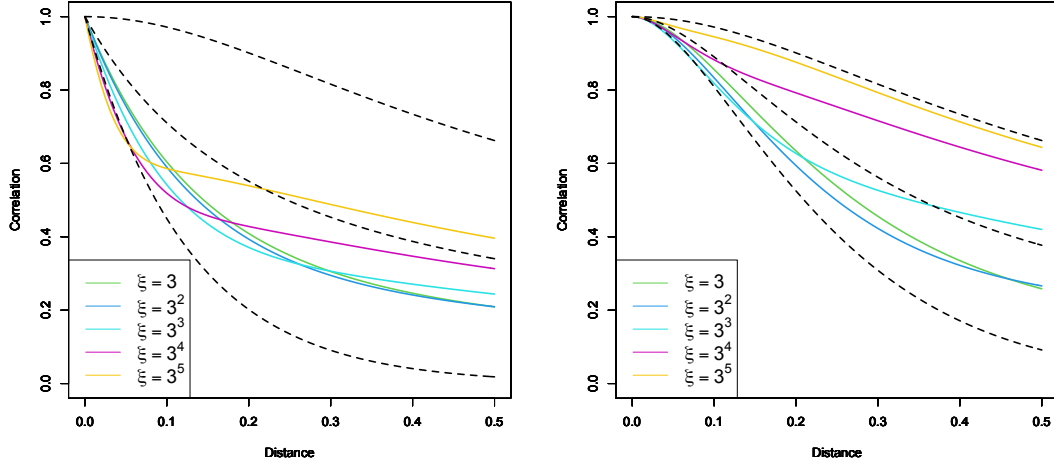


Figure 3.1: Parsimonious hybrid Cauchy-Matérn model for  $\omega = 1/2$ ,  $\alpha = 1/8$ ,  $\nu_1 = 3/4$  and different values of  $\xi$ . (Left)  $\nu_2 = 1/2$  and (Right)  $\nu_2 = 3/2$ . The dashed lines represent the purely Cauchy, purely Matérn, and their average. All the models have been appropriately rescaled in order to obtain correlation functions.

where

$$\tilde{\varphi}_{\mathcal{H}}^{(1)}(h; \boldsymbol{\lambda}_1, \xi_1, \boldsymbol{\vartheta}) = \frac{\tau}{\Gamma(\nu_1)} \Gamma\left(\nu_1; \frac{1}{4\xi_1\alpha_1^2}; \frac{\eta h^2}{4\alpha_1^2}\right) - \frac{1}{\Gamma(\nu_1)} \Gamma\left(\nu_1; \frac{1}{4\xi_1\alpha_1^2}; \frac{h^2}{4\alpha_1^2}\right), \quad (3.12)$$

and  $\tilde{\varphi}_{\mathcal{M}}^{(2)}$  as in (3.6). Then,  $\tilde{\varphi}_{\mathcal{H}\mathcal{M}}$  is positive definite in  $\mathbb{R}^d$  if and only if  $1 < \eta < \tau^{2/d}$ .

**Proof 3.3.** We consider the construction (3.3), with both  $g_1$  and  $g_2$  of the form (3.8), and  $\phi_2$  of Gaussian type. Thus, the derivation of  $\tilde{\varphi}_{\mathcal{M}}^{(2)}$  follows the same arguments employed in the proof of Proposition 3.1.

Before deriving (3.12), let us introduce the following lemma, which is a combination of Corollaries 4, 8 and 11 in Posa (2022).

**Lemma 3.1.** The mapping  $h \mapsto A \exp(-ah^2) - B \exp(-bh^2)$  is positive definite in  $\mathbb{R}^d$  if and only if

$$1 < \frac{a}{b} < \left(\frac{A}{B}\right)^{2/d}. \quad (3.13)$$

Although Posa (2022) focused on dimensions  $d \leq 3$ , the same proof can be used in arbitrary dimensions. To obtain the expression (3.12), we take the following covariance kernel in the first segment of the scale mixture

$$\phi_1(h; u, \boldsymbol{\vartheta}) = \tau \exp(-u\eta h^2) - \exp(-uh^2), \quad h \geq 0. \quad (3.14)$$

Lemma 3.1 ensures that (3.14) is positive definite in  $\mathbb{R}^d$ , provided that  $u > 0$  and  $1 < \eta < \tau^{2/d}$ . Thus,

$$\tilde{\varphi}_{\mathcal{H}}^{(1)}(h; \boldsymbol{\lambda}_1, \xi_1, \boldsymbol{\vartheta}) = \tau \int_0^{\xi_1} \exp(-u\eta h^2) g_{\mathcal{M}}(u; \boldsymbol{\lambda}_1) du - \int_0^{\xi_1} \exp(-uh^2) g_{\mathcal{M}}(u; \boldsymbol{\lambda}_1) du. \quad (3.15)$$



Finally, we invoke the identity (3.9), and we apply it to each integral involved in the right hand side of Equation (3.15).  $\square$

The covariance function (3.14) always takes negative values (Posa, 2022), so it is a natural building block to achieve hybrid models with hole effect. The parameters in  $\boldsymbol{\vartheta}$  are responsible for the sharpness of the hole effect. More precisely, as  $\eta$  approaches  $\tau^{2/d}$ , the hole effect is more pronounced because the positive term in the right hand side of (3.14) has less dominance. Moreover, when  $d = 1$ , we have the least restrictive condition on  $\eta$ , and the resulting hole effect is more marked. It is well known that the possibility of significant negative correlations vanishes as the dimension increases (see, e.g., page 45 in Stein, 1999).

The next proposition characterizes the local attributes of (3.11) and provides a lower bound for this model.

**Proposition 3.4.** Let  $Z$  be a Gaussian random field with covariance function of the form (3.11). Then,  $Z$  is  $\kappa$ -times mean square differentiable if and only if  $\nu_2 > \kappa \geq 0$ . Moreover, we have the lower bound

$$\tilde{\varphi}_{\mathcal{HM}}(h; \boldsymbol{\lambda}, \boldsymbol{\omega}, \boldsymbol{\xi}, \boldsymbol{\vartheta}) \geq \omega_1 (\tau\eta)^{-1/(\eta-1)} \left( \frac{1-\eta}{\eta} \right) \left( 1 - \frac{\gamma(\nu_1; \alpha_1/\xi_1)}{\Gamma(\nu_1)} \right), \quad h \geq 0. \quad (3.16)$$

**Proof 3.4.** The fact that  $\nu_2$  controls the mean square differentiability is a direct consequence of the arguments used in the proof of Proposition 3.2. On the other hand, to find a lower bound, we note that

$$\begin{aligned} \tilde{\varphi}_{\mathcal{HM}}(h; \boldsymbol{\lambda}, \boldsymbol{\omega}, \boldsymbol{\xi}, \boldsymbol{\vartheta}) &\geq \omega_1 \inf_{h \geq 0} \tilde{\varphi}_{\mathcal{H}}^{(1)}(h; \boldsymbol{\lambda}_1, \xi_1, \boldsymbol{\vartheta}) + \omega_2 \inf_{h \geq 0} \tilde{\varphi}_{\mathcal{M}}^{(2)}(h; \boldsymbol{\lambda}_2, \xi_2) \\ &= \omega_1 \int_0^{\xi_1} \inf_{h \geq 0} \phi_1(h; u, \boldsymbol{\vartheta}) g_1(u; \boldsymbol{\lambda}_1) du. \end{aligned}$$

A straightforward calculation shows that  $\phi_1$  attains its minimum value at  $h^* = \sqrt{\frac{\log(\tau\eta)}{u(\eta-1)}}$ . Thus,

$$\phi_1(h; u, \boldsymbol{\vartheta}) \geq \phi_1(h^*; u, \boldsymbol{\vartheta}) = \tau \exp\left(-\frac{\eta \log(\tau\eta)}{\eta-1}\right) - \exp\left(-\frac{\log(\tau\eta)}{\eta-1}\right) = (\tau\eta)^{-1/(\eta-1)} \left( \frac{1-\eta}{\eta} \right).$$

Since  $g_1$  is given by (3.8), we invoke the formula of the cumulative distribution function of an inverse gamma random variable to establish that

$$\int_0^{\xi_1} g_1(u; \boldsymbol{\lambda}_1) du = 1 - \frac{\gamma(\nu_1; \alpha_1/\xi_1)}{\Gamma(\nu_1)}.$$

The proof is completed.  $\square$

Note that as  $\xi_1 \rightarrow \infty$  (i.e., as the hole effect predominates), the lower bound in Equation (3.16) decreases to  $(\tau\eta)^{-1/(\eta-1)}(1-\eta)/\eta$ . On the contrary, as  $\xi_1 \rightarrow 0$ , such a bound increases to zero, i.e., the hole effect becomes negligible, which is not surprising, because in such a case the Matérn class is predominant. A similar conclusion can be obtained in the limit case  $\eta \rightarrow 1$ .

A parsimonious variant of this model consists of taking  $\omega_1 = \omega_2 = \omega$  (variance parameter),  $\alpha_1 = \alpha_2 = \alpha$  (scale parameter) and  $\nu_1 = \nu_2 = \nu$  (smoothness parameter), whereas  $\boldsymbol{\vartheta}$  regulates the hole effect (as discussed above) and  $\xi_1 = \xi_2 = \xi$  has a similar interpretation as in the hybrid Cauchy-Matérn model.

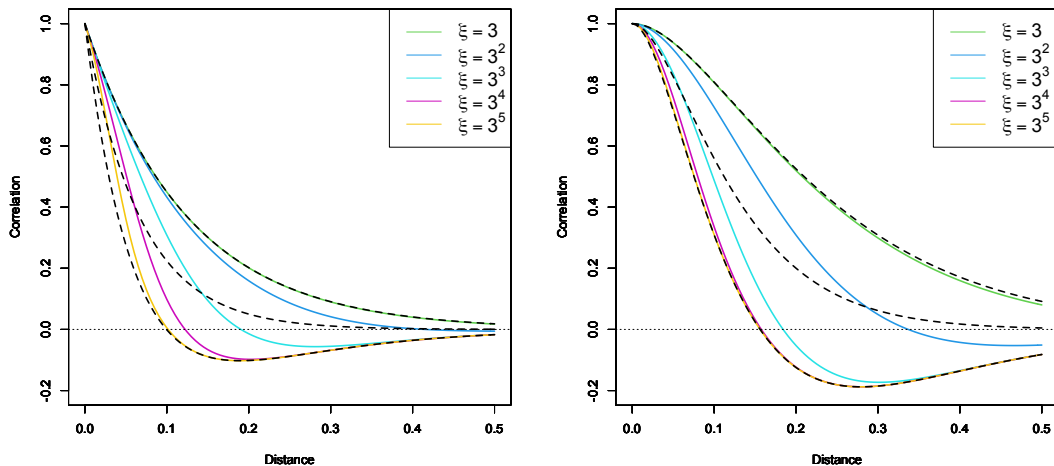


Figure 3.2: Parsimonious hybrid Hole-Effect-Matérn model in dimension one, for  $\omega = 1/2$ ,  $\alpha = 1/8$ ,  $\tau = 2$ ,  $\eta = 7/2$  and different values of  $\xi$ . (Left)  $\nu = 1/2$  and (Right)  $\nu = 3/2$ . The dashed lines represent the limit cases reported in Remark 3.1. All the models have been appropriately rescaled in order to obtain correlation functions.

Figure 3.2 shows the parsimonious hybrid Hole-Effect-Matérn model for different values of  $\xi$ . The limit cases described in Remark 3.1 are also reported, in a similar fashion to Figure 3.1. It can be seen that negative values coexist with different levels of smoothness at the origin, as expected.

## 4 Numerical Experiments

### 4.1 Simulated Data

We conduct simulation studies to assess the performance of maximum likelihood inference when a hybrid covariance structure is present. We focus on the parsimonious hybrid Cauchy-Matérn dependence structure, as it will be applied to real data in the next section. We consider  $\omega = 1$ ,  $\alpha = 1/8$ ,  $\nu_1 = 3/4$  and the following scenarios for  $[\nu_2, \xi]$ : (a)  $[1/2, 40]$ , (b)  $[1/2, 120]$ , (c)  $[3/2, 40]$  and (d)  $[3/2, 120]$ . For each scenario, we simulate 200 independent realizations of a Gaussian random field on 100 uniformly sampled points in the square  $[0, 3]^2$  and estimate the parameters through maximum likelihood. We then repeat the experiment with 256 spatial locations. We only estimate  $\omega$ ,  $\alpha$  and  $\xi$ , whereas  $\nu_1$  and  $\nu_2$  are fixed, which is a common practice in geostatistics. Instead of directly estimating  $\xi$ , we consider the following alternative parameterization:  $\tilde{\xi} = \sqrt{\xi}\alpha$ , which seems to be a natural choice according to Equations (3.5) and (3.6).

Figure 4.1 displays the results. The estimates are approximately unbiased and the variance decreases as the sample size increases from 100 to 256, which is an expected behaviour. The variability of the estimates substantially decreases in scenarios (c) and (d), i.e., when the random field is smoother, which is a typical attribute of likelihood-based estimates in this context (Bevilacqua and Gaetan, 2015). On the contrary, such a variability deteriorates as  $\xi$  increases from 40 to 120. Figure 4.2 shows the log-likelihood in terms of  $\xi$  and  $\alpha$ , with fixed  $\omega$ , for a single realization of the random field, under scenario (b). Although the surface has a clear maximum value, the objective function is apparently more flat in the direction of  $\xi$ . This could explain the increased variability

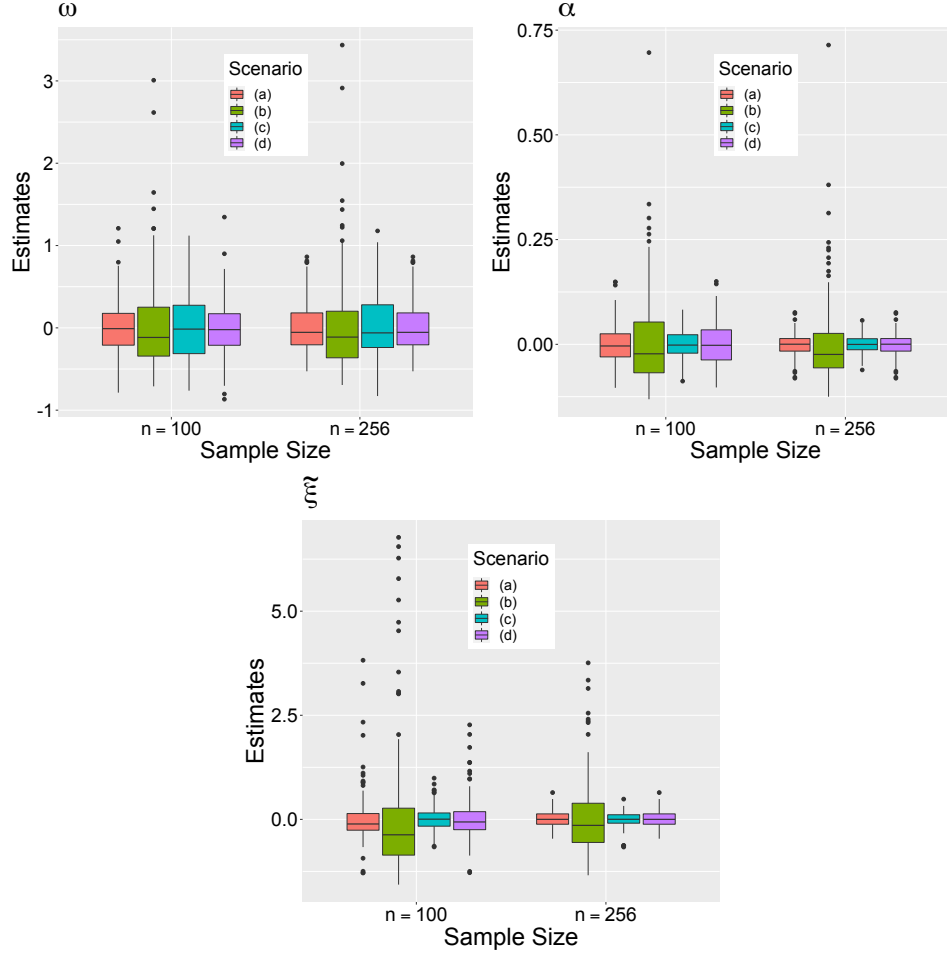


Figure 4.1: Centered boxplots of the maximum likelihood estimates for the parsimonious hybrid Cauchy-Matérn model in scenarios (a)-(d).

in scenarios (b) and (d), with respect to (a) and (c). Despite the previous remarks, in general, the estimates appear to be reasonable in each scenario and no identifiability issues are observed.

We now explore the predictive performance of the proposed class through a cross validation analysis. We simulate 200 independent realizations on 100 uniformly sampled locations in  $[0, 3]^2$  according to the scenarios (a)-(d) described above. We assess the accuracy through a leave-one-out prediction strategy in terms of the mean squared error (MSE), mean absolute error (MAE), log-score (LSCORE) and continuous ranked probability score (CRPS) (see Zhang and Wang, 2010). Small values of these indicators suggest superior predictions. We evaluate the performance of the hybrid Cauchy-Matérn model, using the Generalized Cauchy class as benchmark. Thus, for each realization, we estimate the parameters with both models and proceed to make the predictions through a simple kriging approach. The Generalized Cauchy model (2.4) has been augmented with a multiplicative parameter  $\omega$ , namely  $h \mapsto \omega(1+h^\delta/\alpha)^{-\nu/\delta}$ , so it is parameterized by  $\omega$  and  $\alpha$ , and  $\nu = 3/4$  and  $\delta = 1, 2$  are fixed.

Table 4.1 shows that, in each scenario, the proposed hybrid model outperforms its competitor. All the cross-validation scores substantially decrease in scenarios (c) and (d). From this brief study, we observe that when the true underlying covariance has a hybrid structure, an incorrect specification

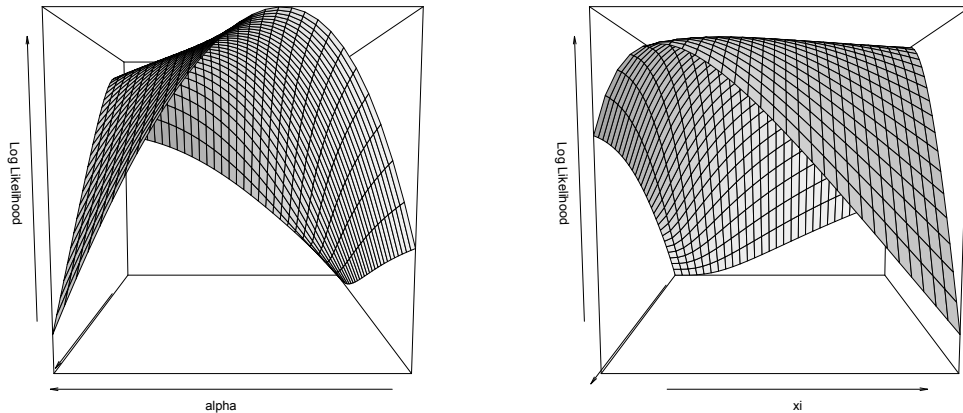


Figure 4.2: Log-likelihood function, with respect to  $\alpha$  and  $\xi$ , for scenario (b). Left and right panels correspond to the same plot from different viewpoints.

of the spatial association has a negative impact on the posterior predictions. Since the behaviour of an isotropic covariance function near the origin has a strong impact on the quality of predictions (Stein, 1999), our simulation experiment suggests that in some circumstances the local shape of the proposed model cannot be replicated by other appealing existing structures.

## 4.2 A Real Data Illustration

The estimation of recoverable resources is a task of fundamental importance in modern mining processes. A sound evaluation of such resources is crucial from an economic viewpoint and is critical for assessing the long-term availability of mineral resources and its impact on society. We consider a data set from a lateritic nickel deposit mined by open pit in Colombia, which contains measurements of the grades of nickel, iron, chrome, alumina, magnesia and silica.

This study focuses on nickel concentrations that are placed at an elevation of about 120 meters, where 199 irregularly spaced observations are available. We apply a log-transformation to reduce the skewness, and then the sample mean is subtracted. The resulting values are approximately Gaussian. The left panel of Figure 4.4 shows the transformed data set. We fit two covariance models: the former is the parsimonious hybrid Cauchy-Matérn, parameterized by  $\omega$ ,  $\alpha$  and  $\tilde{\xi}$ , with fixed  $\nu_1 = 1/4$  and  $\nu_2 = 1/2$ , and the latter is the Generalized Cauchy, parameterized as in Section 4.1, with fixed  $\nu = 1/4$  and  $\delta = 0.95$ . The values of the fixed parameters have been selected after some experimental trials, taking into account the local behavior of the sample covariance (see Figure 4.3).

Table 4.2 reports the likelihood estimates, with the corresponding standard errors, and the Akaike information criterion (AIC). We observe that the hybrid Cauchy-Matérn model outperforms its competitor in terms of AIC. Figure 4.3 shows that the fitted covariance models seem to be reasonably close to the sample covariance. The fitted models differ substantially near the origin (distances less than 3 meters), since the hybrid model decays faster. On the contrary, for larger distances the hybrid model decays slower, although the difference between the curves becomes slight for distances greater than 15 meters.

Table 4.1: Cross-validation scores for the parsimonious hybrid Cauchy-Matérn and Generalized Cauchy (with  $\delta = 1, 2$ ) models in scenarios (a)-(d).

Scenario	Model	MSE	MAE	LSCORE	CRPS
(a)	Hybrid Cauchy-Matérn	0.706	0.668	1.231	1.773
	Generalized Cauchy ( $\delta = 1$ )	0.714	0.672	1.238	1.787
	Generalized Cauchy ( $\delta = 2$ )	0.718	0.674	1.241	1.798
(b)	Hybrid Cauchy-Matérn	0.480	0.549	1.034	1.462
	Generalized Cauchy ( $\delta = 1$ )	0.489	0.555	1.046	1.480
	Generalized Cauchy ( $\delta = 2$ )	0.497	0.559	1.055	1.506
(c)	Hybrid Cauchy-Matérn	0.172	0.316	0.398	0.840
	Generalized Cauchy ( $\delta = 1$ )	0.176	0.319	0.446	0.851
	Generalized Cauchy ( $\delta = 2$ )	0.176	0.319	0.414	0.862
(d)	Hybrid Cauchy-Matérn	0.075	0.210	0.024	0.561
	Generalized Cauchy ( $\delta = 1$ )	0.077	0.213	0.052	0.575
	Generalized Cauchy ( $\delta = 2$ )	0.082	0.219	0.103	0.612

Table 4.2: Parameter estimates and Akaike Information Criterion (AIC) of fitted covariance models. Standard errors are reported in parentheses.

Model	$\omega$	$\alpha$	$\tilde{\xi}$	AIC
Hybrid Cauchy-Matérn	1.055 (0.2516)	12.31 (2.801)	0.063 (0.042)	-34.03
Generalized Cauchy	0.164 (0.040)	1.959 (0.849)	- -	-31.93

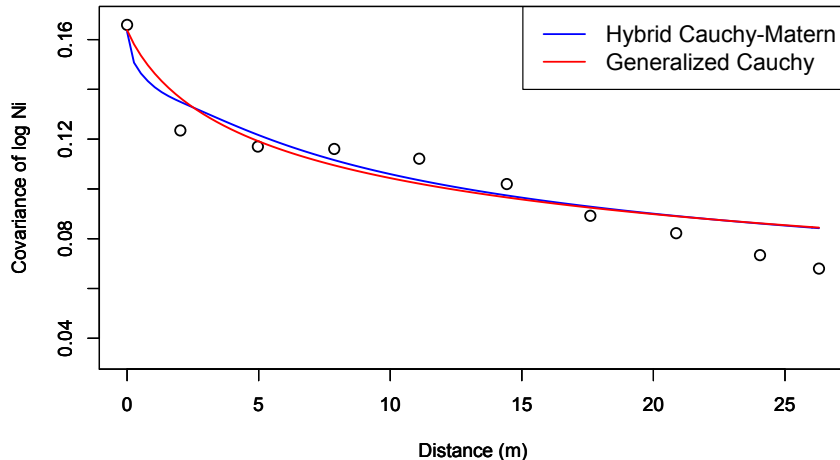


Figure 4.3: Sample (circles) and modeled (solid lines) covariances of log-nickel concentrations.

Table 4.3: Scores for the leave-one-out cross-validation study of log-nickel concentrations.

Model	MSE	MAE	LSCORE	CRPS
Hybrid Cauchy-Matérn	0.0428	0.1431	-0.1840	0.4113
Generalized Cauchy	0.0443	0.1462	-0.1677	0.4159

In order to compare the models in terms of predictive performance, we conduct a cross-validation study, in a similar fashion to the experiments performed with simulated data. Table 4.3 shows evidence, based on a leave-one-out cross-validation scheme, that the hybrid model has a better performance for this specific data set. In percentage terms, the MSE shows an improvement of approximately 3.4%. The largest difference occurs when we compare the LSCORE's (about 9% improvement).

We conclude this section with an illustration of a downscaled map of log-nickel concentrations (see Figure 4.4), using the hybrid Cauchy-Matérn model. The interpolated spatial map, which is obtained through simple kriging, is exhibited on a spatial grid of approximately 1 meter (7500 locations). This kriged surface could be useful in small-scale mining processes, as it is a crucial step for industrial exploration and to quantify mineral reserves.

## 5 Conclusions and Perspectives

We introduced a simple formalism to build sophisticated parametric families of covariance functions. We focused on a combination between the Matérn and Cauchy models, where local (mean square differentiability) and global (long memory) properties coexist in a single family. We have also illustrated the use of our methodology by constructing a model that behaves as the Matérn class at short distances and attains negative values at large distances. Simulation studies show that a parsimonious hybrid Cauchy-Matérn model has statistically identifiable parameters. Also, this model provides improvements in terms of predictive performance in comparison to existing models,

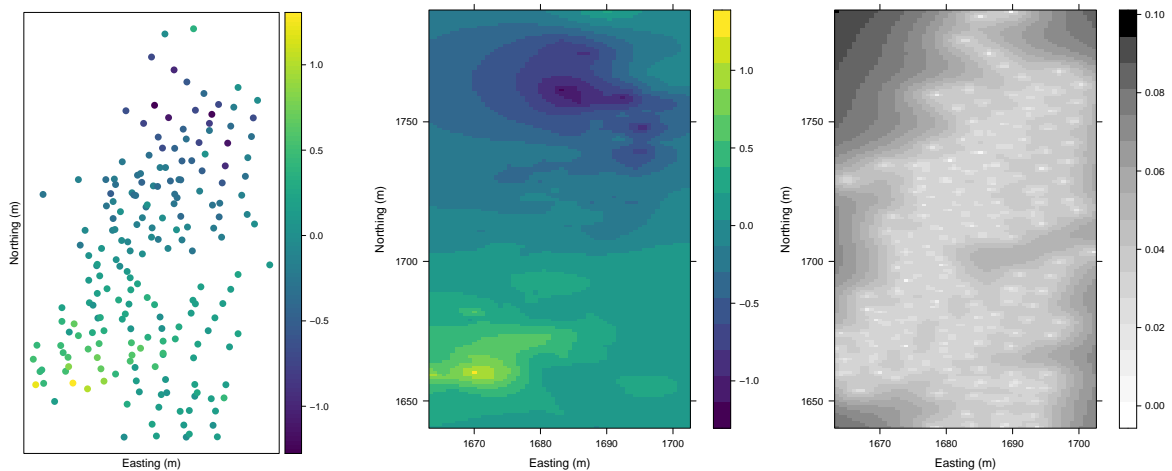


Figure 4.4: Log-nickel concentrations (left), with the kriged surface (middle) and the corresponding variance (right).

when a hybrid inherent dependence structure is present. We reach similar conclusions when we apply this methodology to a mining dataset. While similar numerical studies could be performed for the hybrid Hole-Effect-Matérn model, we avoid them for the sake of simplicity and brevity. Additional interesting extensions of this work can be tackled in future investigations. We now provide two concrete research lines that could emerge from this work.

## Multivariate Hybrid Covariance Models

In many practical situations, two or more variables are simultaneously recorded. Thus, our findings can be generalized to the case of multivariate fields  $\{\mathbf{Z}(\mathbf{s}) = (Z_1(\mathbf{s}), \dots, Z_p(\mathbf{s}))^\top, \mathbf{s} \in \mathbb{R}^d\}$ , having an isotropic matrix-valued covariance function  $\Phi : [0, \infty) \rightarrow \mathbb{R}^{p \times p}$ , that is,  $\text{cov}[Z_i(\mathbf{s}), Z_j(\mathbf{s}')] = \Phi_{ij}(h)$ ,  $h \geq 0$ , where  $h = \|\mathbf{s} - \mathbf{s}'\|$  and  $i, j = 1, \dots, p$ . We propose the hybrid model

$$\tilde{\Phi}(h; \boldsymbol{\lambda}, \boldsymbol{\omega}, \boldsymbol{\xi}) = \omega_1 \int_0^{\xi_1} \exp(-uh^2) \mathbf{G}_1(u; \boldsymbol{\lambda}_1) du + \omega_2 \int_{\xi_2}^{\infty} \exp(-uh^2) \mathbf{G}_2(u; \boldsymbol{\lambda}_2) du,$$

that generalizes (3.1), where the vectors of parameters  $\boldsymbol{\lambda}_i$  must be chosen in such a way that the  $p \times p$  matrices  $\mathbf{G}_i(u; \boldsymbol{\lambda}_i)$  are positive semi-definite for every fixed  $u \geq 0$ . Hence, a straight application of Proposition 4 in Porcu and Zastavnyi (2011) would ensure  $\tilde{\Phi}$  to be positive semi-definite. A multivariate version of the hybrid Cauchy-Matérn covariance function is a natural candidate. The works of Gneiting et al. (2010) and Moreva and Schlather (2022) are relevant to tackle this challenge. A multivariate version of the formulation (3.3) could be deduced similarly.

## Hybrid Covariance Models on Spheres

For random fields that are indexed by the  $d$ -dimensional unit sphere,  $\mathbb{S}^d$ , which is a useful framework when analyzing global data ( $\mathbb{S}^2$  is used as an approximation of the Earth), the isotropy assumption is given by  $\text{cov}[Z(\mathbf{s}), Z(\mathbf{s}')] = \psi(\theta)$ ,  $\mathbf{s}, \mathbf{s}' \in \mathbb{S}^d$ , where  $\psi : [0, \pi] \rightarrow \mathbb{R}$  is a continuous mapping and  $\theta = \arccos(\mathbf{s}^\top \mathbf{s}') \in [0, \pi]$  is the geodesic distance. Schoenberg's characterization (Schoenberg, 1942) establishes that a parametric isotropic covariance function  $\psi(\cdot; \boldsymbol{\lambda})$  is valid in any dimension  $d$ , if

and only if, it can be written as  $\psi(\theta; \boldsymbol{\lambda}) = \sum_{\ell=0}^{\infty} \beta_{\ell}(\boldsymbol{\lambda})(\cos \theta)^{\ell}$ ,  $\theta \in [0, \pi]$ , for some nonnegative and summable parametric sequence  $\{\beta_{\ell}(\boldsymbol{\lambda})\}_{\ell=0}^{\infty}$ . Thus, the hybrid models can be adapted to the spherical context by considering a modified sequence of the form

$$\tilde{\beta}_{\ell}(\boldsymbol{\lambda}, \boldsymbol{\omega}, \boldsymbol{\xi}) = \omega_1 \beta_{\ell}^{(1)}(\boldsymbol{\lambda}_1) 1_{[0, \lfloor \xi_1 \rfloor]}(\ell) + \omega_2 \beta_{\ell}^{(2)}(\boldsymbol{\lambda}_2) 1_{[\lfloor \xi_2 \rfloor, \infty)}(\ell), \quad \ell = 0, 1, \dots,$$

where  $\lfloor \xi_i \rfloor \geq 0$ , for  $i = 1, 2$ , with  $\lfloor \cdot \rfloor$  standing for the floor function, and  $\beta_{\ell}^{(i)}$  being a nonnegative and summable sequence. The local properties of spherically indexed random fields, and their connections with the covariance function, have been studied in past literature (Bingham, 1973; Guinness and Fuentes, 2016). However, global properties such as long memory are less intuitive in this scenario as the spatial domain is a compact set. Covariance functions with hole effect, for low-dimensional spheres, could be obtained by adapting formulation (3.3).

## Acknowledgements

Alfredo Alegría was partially supported by the National Agency for Research and Development of Chile, through grant ANID/FONDECYT/INICIACIÓN/No. 11190686. Fabián Ramirez was partially supported by the Dirección de Postgrados y Programas (DPP) of the Universidad Técnica Federico Santa María. Emilio Porcu is supported by the Khalifa University of Science and Technology under Award No. FSU-2021-016.

## References

- Abramowitz, M. and Stegun, I. A. (1972). *Handbook of Mathematical Functions with Formulas, Graphs, and Mathematical Tables*. Dover Publications.
- Alegría, A. (2020). Cross-dimple in the cross-covariance functions of bivariate isotropic random fields on spheres. *Stat*, 9(1):e301.
- Alegría, A., Emery, X., and Porcu, E. (2021). Bivariate Matérn covariances with cross-dimple for modeling coregionalized variables. *Spatial Statistics*, 41:100491.
- Barndorff-Nielsen, O. (1978). Hyperbolic distributions and distributions on hyperbolae. *Scandinavian Journal of Statistics*, 5(3):151–157.
- Barp, A., Oates, C. J., Porcu, E., and Girolami, M. (2022). A Riemann–Stein kernel method. *Bernoulli*, 28(4):2181–2208.
- Berg, C., Mateu, J., and Porcu, E. (2008). The Dagum family of isotropic correlation functions. *Bernoulli*, 14(4):1134–1149.
- Bevilacqua, M., Caamaño-Carrillo, C., and Porcu, E. (2022). Unifying compactly supported and Matérn covariance functions in spatial statistics. *Journal of Multivariate Analysis*, 189:104949.
- Bevilacqua, M. and Gaetan, C. (2015). Comparing composite likelihood methods based on pairs for spatial Gaussian random fields. *Statistics and Computing*, 25(5):877–892.
- Bingham, N. H. (1973). Positive Definite Functions on Spheres. *Proc. Cambridge Phil. Soc.*, 73:145–156.
- Chaudhry, M. A. and Zubair, S. M. (1994). Generalized incomplete gamma functions with applications. *Journal of Computational and Applied Mathematics*, 55(1):99–123.



- Chen, W., Castruccio, S., Genton, M. G., and Crippa, P. (2018). Current and future estimates of wind energy potential over Saudi Arabia. *Journal of Geophysical Research: Atmospheres*, 123(12):6443–6459.
- Chilès, J.-P. and Delfiner, P. (2012). *Geostatistics: Modeling Spatial Uncertainty, Second Edition*. John Wiley & Sons.
- Cockayne, J., Oates, C. J., Sullivan, T. J., and Girolami, M. (2019). Bayesian probabilistic numerical methods. *SIAM review*, 61(4):756–789.
- Cressie, N. (1993). *Statistics for Spatial Data*. Wiley, New York, revised edition.
- Cressie, N. and Kornak, J. (2003). Spatial Statistics in the Presence of Location Error with an Application to Remote Sensing of the Environment. *Statistical Science*, 18(4):436–456.
- Daley, D. and Porcu, E. (2014). Dimension walks and Schoenberg spectral measures. *Proceedings of the American Mathematical Society*, 142(5):1813–1824.
- Di Lorenzo, E., Combes, V., Keister, J., Strub, P., Andrew, T., Peter, F., Marck, O., Furtado, J. ., Bracco, A., Bograd, S., Peterson, W., Schwing, F., Taguchi, B., Hormázabal, S., and Parada, C. (2014). Synthesis of Pacific Ocean Climate and ecosystem dynamics. *Oceanography*, 26(4):68–81.
- Edwards, M., Castruccio, S., and Hammerling, D. (2019). A multivariate Global Spatio-Temporal Stochastic Generator for Climate Ensembles. *Journal of Agricultural, Biological and Environmental Sciences*.
- Emery, X. and Lantuéjoul, C. (2006). Tbsim: A computer program for conditional simulation of three-dimensional gaussian random fields via the turning bands method. *Computers & Geosciences*, 32(10):1615–1628.
- Emery, X. and Séguret, S. A. (2020). *Geostatistics for the Mining Industry: Applications to Porphyry Copper Deposits*. CRC Press.
- Furrer, R., Genton, M. G., and Nychka, D. (2006). Covariance tapering for interpolation of large spatial datasets. *Journal of Computational and Graphical Statistics*, 15(3):502–523.
- Furrer, R., Sain, S. R., Nychka, D., and Meehl, G. A. (2007). Multivariate bayesian analysis of atmosphere–ocean general circulation models. *Environmental and Ecological Statistics*, 14(3):249–266.
- Gneiting, T., Kleiber, W., and Schlather, M. (2010). Matérn cross-covariance functions for multivariate random fields. *Journal of the American Statistical Association*, 105:1167–1177.
- Gneiting, T. and Schlather, M. (2004). Stochastic models that separate fractal dimension and the Hurst effect. *SIAM review*, 46(2):269–282.
- Gradshteyn, I. and Ryzhik, I. (2007). *Table of Integrals, Series, and Products*. Academic Press, Amsterdam, 7th. edition.
- Guinness, J. and Fuentes, M. (2016). Isotropic covariance functions on spheres: Some properties and modeling considerations. *Journal of Multivariate Analysis*, 143:143–152.
- Guinness, J. and Hammerling, D. (2018). Compression and conditional emulation of climate model output. *Journal of the American Statistical Association*, 113(521):56–67.
- Hristopulos, D. T. (2020). *Random fields for spatial data modeling*. Springer.

- James, G., Witten, D., Hastie, T., and Tibshirani, R. (2013). *An introduction to statistical learning*, volume 112. Springer.
- Kaufman, C. G., Schervish, M. J., and Nychka, D. W. (2008). Covariance tapering for likelihood-based estimation in large spatial data sets. *Journal of the American Statistical Association*, 103(484):1545–1555.
- Laga, I. and Kleiber, W. (2017). The modified Matérn process. *Stat*, 6(1):241–247.
- Ma, P. and Bhadra, A. (2022). Beyond Matérn: On a Class of Interpretable Confluent Hypergeometric Covariance Functions. *Journal of the American Statistical Association*, (in press).
- Matérn, B. (1986). *Spatial Variation — Stochastic Models and Their Application to Some Problems in Forest Surveys and Other Sampling Investigations*. Springer.
- Moreva, O. and Schlather, M. (2022). Bivariate covariance functions of Pólya type. *Journal of Multivariate Analysis*, in press.
- Ostoja-Starzewski, M. (2006). Material spatial randomness: From statistical to representative volume element. *Probabilistic engineering mechanics*, 21(2):112–132.
- Pazouki, M. and Schaback, R. (2011). Bases for kernel-based spaces. *Journal of Computational and Applied Mathematics*, 236(4):575–588.
- Porcu, E., Alegria, A., and Furrer, R. (2018a). Modeling temporally evolving and spatially globally dependent data. *International Statistical Review*, 86(2):344–377.
- Porcu, E., Bevilacqua, M., and Hering, A. S. (2018b). The Shkarofsky-Gneiting class of covariance models for bivariate Gaussian random fields. *Stat*, 7(1):e207.
- Porcu, E. and Zastavnyi, V. (2011). Characterization theorems for some classes of covariance functions associated to vector valued random fields. *Journal of Multivariate Analysis*, 102(9):1293–1301.
- Posa, D. (2022). Special classes of isotropic covariance functions. *Preprint, Research Square*.
- Schaback, R. and Wendland, H. (2006). Kernel techniques: from machine learning to meshless methods. *Acta numerica*, 15:543–639.
- Schlather, M. (2010). Some covariance models based on normal scale mixtures. *Bernoulli*, 16(3):780–797.
- Schlather, M. and Moreva, O. (2017). A parametric model bridging between bounded and unbounded variograms. *Stat*, 6(1):47–52.
- Schoenberg, I. J. (1938). Metric Spaces and Completely Monotone Functions. *Annals of Mathematics*, 39(4):811–841.
- Schoenberg, I. J. (1942). Positive definite functions on spheres. *Duke Mathematical Journal*, 9(1):96–108.
- Stein, M. L. (1999). *Statistical Interpolation of Spatial Data: Some Theory for Kriging*. Springer, New York.
- Stein, M. L. (2007). Spatial variation of total column ozone on a global scale. *The Annals of Applied Statistics*, 1(1):191–210.

Yaglom, A. M. (1987). *Correlation Theory of Stationary and Related Random Functions, Volume I: Basic Results*, volume 131. Springer.

Zhang, H. and Wang, Y. (2010). Kriging and cross-validation for massive spatial data. *Environmetrics*, 21(3-4):290–304.